Journal of Medicinal Chemistry

Volume 49, Number 5 March 9, 2006

Letters

Selective Irreversible Inhibition of Fructose 1,6-Bisphosphate Aldolase from *Trypanosoma brucei*

Chantal Dax,[†] Francis Duffieux,[‡,#] Nicolas Chabot,[†] Mathieu Coincon,[§] Jurgen Sygusch,[§] Paul A. M. Michels,[‡] and Casimir Blonski*,[†]

LSPCMIB, UMR-CNRS 5068, Groupe de Chimie Organique Biologique, Université Paul Sabatier, Bat. IIR1, 118 Route de Narbonne 31062, Toulouse Cedex 9, France, Department of Biochemistry, University of Montreal, Pavillon Roger Gaudry, CP 6128, Station Centre Ville, Montréal, QC, Canada, H3C 3J7, and Research Unit for Tropical Diseases, Christian de Duve Institute of Cellular Pathology, and Laboratory of Biochemistry, Université Catholique de Louvain, ICP-TROP 74-39, Avenue Hippocrate 74, B-1200 Brussels, Belgium

Received March 15, 2005

Abstract: An irreversible competitive inhibitor hydroxynaphthaldehyde phosphate was synthesized that is highly selective against the glycolytic enzyme fructose 1,6-bisphosphate aldolase from *Trypanosoma brucei* (causative agent of sleeping sickness). Inhibition involves Schiff base formation by the inhibitor aldehyde with Lys116 followed by reaction of the resultant Schiff base with a second residue. Molecular simulations indicate significantly greater molecular geometries conducive for nucleophilic attack in *T. brucei* aldolase than the mammalian isozyme and suggest Ser48 as the Schiff base modifying residue.

Among the many diseases that afflict humankind, those caused by protozoan parasites occupy an important place because of the large number of victims, the lack of efficient therapy, and their continuing spread. The World Health Organization reported 55 000 deaths in 2002 out of 500 000 cases for sleeping sickness in sub-Saharan Africa, caused by infection with *Trypanosoma brucei*.[1] Trypanosomiasis also significantly affects human nutrition through their impact on food animals by killing 3 million cattle per year. A number of drugs have been used in the treatment of trypanosomal infections (Figure 1).

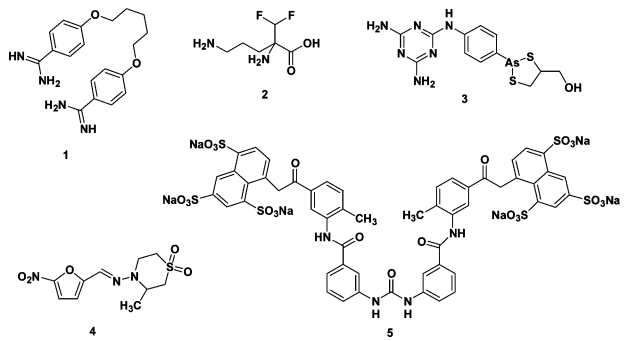

Figure 1. Drugs currently in use to treat trypanosomiasis: **1**, pentamidine; **2**, difluoromethylornithine; **3**, melarsoprol; **4**, nifurtimox; **5**, suramin, sodium salt.

Suramin, pentamidine, and some arsenical drugs often induce severe toxic side effects, and resistance against these drugs is spreading.[2] The drug most recently introduced (early 1990s) against sleeping sickness is (*R,S*)-2-difluoromethylornithine (DFMO, initially developed as an anticancer drug[3]). However, this drug is only active against *Trypanosoma brucei gambiense* (prevalent in west and central Africa) whereas *T. b. rhodesiense* (prevalent in east and southern Africa) is insensitive to this compound.[4] An additional problem is that large amounts of DFMO are required to treat a patient.[5] The need for broad spectrum, inexpensive, highly efficient, and nontoxic drugs therefore remains a priority.

Among the potential metabolic targets considered for the development of new drugs, glycolysis appears as a highly promising pathway, since it is the only ATP-generating process in the bloodstream form of *T. brucei*.[6] It has been shown that trypanosomal glycolysis contains several structural features distinct from the corresponding process in mammalian cells, which may allow for the design of selective compounds without liability in mammals.[7] The approach we considered was to inhibit a glycolytic enzyme with a compound targeting its active site. We chose the fourth enzyme in the cascade as the target, i.e., class I fructose 1,6-bisphosphate aldolase (EC 4.1.2.13). On the basis of the literature[8] and previous work from our

* To whom correspondence should be addressed. Phone: 33561556486. Fax: 33561556011. E-mail: blonski@cict.fr.
[†] Université Paul Sabatier.
[‡] Université Catholique de Louvain.
[#] Present address: Groupe Sanofi Aventis, Protein Production and Engineering, 13, Quai Jules Guesde, BP14 94403 Vitry-sur-Seine Cedex, France.
[§] University of Montreal.

10.1021/jm050237b CCC: $33.50
Published on Web 02/15/2006

Scheme 1. Synthesis of *T. brucei* Aldolase Inhibitor **9**[a]

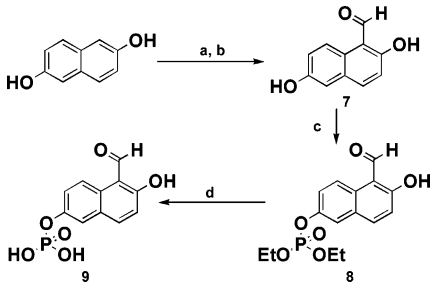

[a] Reagents: (a) biphenylformamidine, acetone, 82% (**6**; see Supporting Information); (b) H_2SO_4, H_2O/ EtOH, 96%; (c) $(EtO)_3P$, I_2, pyridine, CH_2Cl_2/THF, 31%; (d) Me_3SiBr, CH_2Cl_2, H_2O, NaOH, 90%.

Table 1. Interaction of TBK 1 with Rabbit Muscle (RM) and *T. brucei* (Tb) Class I Aldolase

incubation time (min)	**9** (mM)	enzyme (0.2 mg/mL)	residual activity (%)
5	1	RM	80
15			80
5	0.1	RM	100
15			100
5	0.5	Tb	<20
15			0
5	0.02	Tb	75
15			50

laboratory,[9] we envisaged mimics of Schiff base formation (iminium ion) by use of phosphorylated naphthalene derivatives. Such derivatives feature an aldehyde group for Schiff base formation and whose resulting iminium ion is stabilized by the presence of an OH group at the ortho position.[10] Permutation of the three functionalities (phosphate, aldehyde, and hydroxyl) on the naphthalene skeleton allows for the design of lead compounds with different functional topologies.

A number of such compounds were synthesized and assayed on both *T. brucei* and rabbit muscle aldolase. Synthesis of the most promising compound, **9** (TBK1) likely to form a Schiff base with one of the three lysyl groups of the active site (Lys116, -156, and -239 in *T. brucei* aldolase), is shown in Scheme 1.

Synthesis of **9** required, as starting material, 2,6-dihydroxynaphthalene formylated at position 1 using diphenyl formamidine[11] followed by hydrolysis of the resulting Schiff base under acidic conditions to yield the aldehyde derivative **7**. The key step was selective monophosphorylation at position 6 of **7** to obtain the ester derivative **8** without a protecting group at position 2. This was performed using the triethyl phosphite/ pyridine/iodine procedure.[12] Compound **9** was then obtained by the transesterification reaction of **8** using silyltrimethyl bromide and followed by routine hydrolysis.

The effect of **9** on aldolase can be summarized in six points.

(1) The inhibitory effect of **9** was investigated on mammalian and parasite aldolases. Standard conditions were employed for kinetic constant determination (see Supporting Information). A time-dependent inhibition of the *T. brucei* enzyme was observed at low concentration (20 μM) (Table 1) which could not be reversed upon dialysis (see Supporting Information).

Rabbit muscle aldolase by comparison was not inhibited or only very weakly at high inhibitor concentration (1 mM). Compound **9** selectivity was further explored using aldolases from other sources, and the results are summarized in Table 2. In each case, **9** (100 μM) was incubated with enzyme at 0.2 mg/mL. No effect was observed on the mammalian enzymes (rabbit muscle and human liver), whereas the aldolases from three protozoan parasites (*T. brucei*, *Leishmania mexicana*, and *Plasmodium falciparum*) were inhibited, with the strongest effect on *T. brucei* aldolase.

$$E + I \underset{k_2}{\overset{k_1}{\rightleftharpoons}} EI \underset{k_4}{\overset{k_3}{\rightleftharpoons}} EI^*; \quad K_i = \frac{k_2}{k_1}; \quad k_4 = 0$$

Figure 2. Scheme for the interaction kinetics of **9** with *T. brucei* aldolase.

Table 2. Selective Inhibition of Class I Aldolases by **9**

enzyme (0.2 mg/mL)	residual activity (%)
Conditions: 100 μM **9**, 15 min	
rabbit muscle	100
human liver	100
Trypanosoma brucei	<0.5
Leishmania mexicana	15
Plasmodium falciparum	30

Table 3. In Vitro Study of *T. brucei* Aldolase Protection against **9** Inhibition by Its Substrates and Competitive Inhibitors[a]

		residual activity (%) ± 5% at	
compd	concn (mM)	5 min	15 min
none		15	0
DHAP	0.250	56	48
	0.500	63	44
	1	60	52
	10	80	70
FBP	1	80	51
	10	100	89
hexitol 1,6-bisphosphate (HBP)	1	100	100
	0.1	100	100
naphthyl 1,6-bisphosphate (NBP)	1	100	100

[a] *T. brucei* aldolase, 0.2 mg/mL.

Compound **9** appears to be a very selective inhibitor of *T. brucei* aldolase. Further analyses (see Supporting Information) yielded inhibition constants $K_i = 23.03 \pm 2.31$ μM and $k_3 = 0.39 \pm 0.04$ min^{-1} with $k_4 \approx 0$, values indicating a quasi-irreversible behavior by **9** (Figure 2). We therefore concentrated our efforts on *T. brucei* aldolase.

(2) To determine the inhibition mode of **9**, we analyzed the protection of *T. brucei* aldolase against inhibition by its substrates fructose 1,6-P_2 (FBP) and dihydroxyacetone-P (DHAP) and by two strong competitive inhibitors, namely, hexitol-1,6-P_2 (HBP, an FBP analogue resulting from the reduction of the FBP carbonyl group, $K_i = 0.45$ μM)[13] and naphthalene-2,6-P_2 (NBP, $K_i = 0.28$ μM).[8] Compound **9** (100 μM) was incubated with *T. brucei* aldolase and in the presence of different concentrations of substrates (FBP, DHAP) or competitive inhibitors (HBP, NBP). The residual activity was determined after 5 and 15 min of incubation. The results are summarized in Table 3 and are consistent with active site binding. FBP and DHAP only partially protected the enzyme against inhibition. By contrast, both competitive inhibitors, which cannot undergo a retro aldolization reaction, totally protected the enzyme.

(3) To investigate the molecular process by which inhibition occurs, we used UV−vis difference spectroscopy to probe the aldolase−**9** interaction. The spectrum corresponding to the interaction of inhibitor with the *T. brucei* enzyme is shown in Figure 3. Compared to the spectrum of **9** reacting with a lysine mimic, ϵ-aminocaproic acid (Supporting Information), the spectrum for the reaction with the enzyme is different. In both cases, however, the presence of isosbestic points in the spectra indicates that complex formation proceeds without accumulation of intermediates or side reactions.

We hypothesized that **9** inhibition involves initial Schiff base formation with enzyme followed by a nucleophilic attack by a

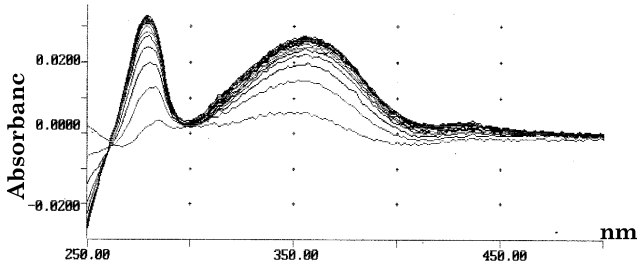

Figure 3. UV−vis difference spectrum of **9**. Reaction of *T. brucei* aldolase (0.2 mg/mL) and **9** (50 μM) in TEA buffer, pH 7, $\Delta t = 2$ min. Absorption spectrum has $\lambda_{max} = 278$ and 356 nm with isosbestic point at 262 nm.

second active site residue. Such a reaction sequence was reported for naphthalene dicarboxaldehyde, which upon Schiff base formation reacts with a cysteine residue.[14] Similarly in the reaction of pyridoxal phosphate with ethane-1,2-diamine,[15] the resulting iminium ion undergoes an intramolecular nucleophilic attack by the second amino group to form a cyclic geminal diamine. To explore such a possibility, we examined the reaction of **9** with model compounds that are mimics of amino acid residues: ethanolamine as a serine analogue, cysteamine as a cysteine mimic, and ethane-1,2-diamine as a second lysyl group. The difference spectrum of the reaction with **9** by ethanolamine resembled closely the spectrum obtained with the enzyme that is shown in Figure 3; resultant absorption maxima (λ_{max} at 270 and 350 nm) and isosbestic point ($\lambda = 255$ nm) were only slightly shifted (~7 nm) toward the UV. We therefore concluded that the amino acid reacting with the intermediate iminium ion formed between the enzyme and **9** is most likely a serine residue. Further support for this conclusion is not inconsistent with the observation below.

(4) The formation of enzyme−inhibitor complexes was studied by electrospray mass spectrometry with the recombinant *L. mexicana* aldolase, which exhibits the same inhibition pattern as the *T. brucei* enzyme (see point 1). Mass spectrometric analyses with the recombinant Trypanosoma protein were unsuccessful. The results obtained with the recombinant *L. mexicana* aldolase corresponded to an observed $\Delta m/z$ of 255 between the free enzyme and the **9**−enzyme complex (see Supporting Information) and indicate a single inhibitor molecule bound per subunit of enzyme. These data are not inconsistent with the formation of the iminium ion concomitant with the loss of a water molecule and that of the putative internal adduct because both have the same mass as the iminium ion intermediate.

(5) To determine which residue was involved in Schiff base formation, point mutations were made of active site lysine residues in the recombinant *T. brucei* enzyme. Active site lysine residues were mutated to methionine, yielding constructs K116M, K156M, and K239M. Compound **9** was incubated with each construct, and the corresponding UV−vis difference spectra were compared to that obtained with the wild-type (Figure 3). For mutants K156M and K239M, the spectra were identical to that of the wild-type enzyme. By contrast, K116M yielded a different spectrum, indicating that Lys116 is the active-site residue responsible for Schiff base formation. This result was corroborated by the observation that the K116M mutant was not inhibited by **9**.

(6) Finally, to gain insight into the preferential reactivity of **9** toward parasite aldolases, we docked it into the crystallographic structures of rabbit muscle and *T. brucei* aldolases, minimized the interaction energies of resulting complexes, and then compared the trajectories of the molecular dynamics

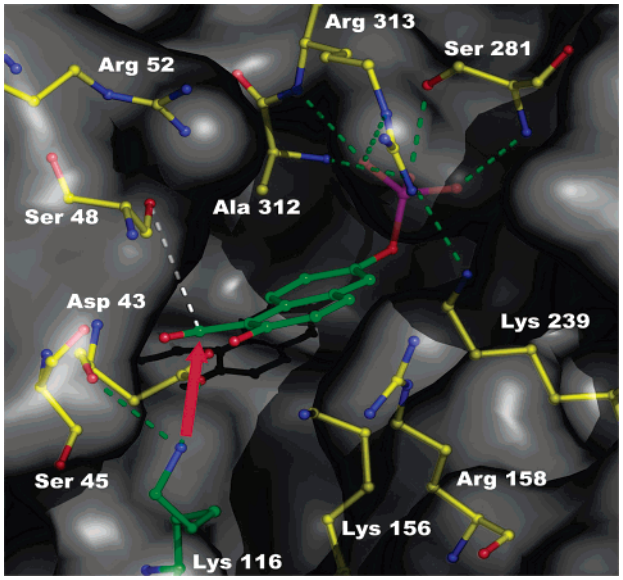

Figure 4. Michaelis complex formed in the *T. brucei* aldolase active site with **9** inhibitor. The solvent-accessible surface of the protein is depicted in gray. Dotted green lines represent hydrogen bonds or electrostatic interactions, and active site residues proximal to **9** are labeled. The red arrow shows the presumed trajectory corresponding to nucleophilic attack by Lys116 Nz on the electrophilic C_7 aldehyde carbon. Lys116 is oriented by two hydrogen bonds made by its Nz atom to carboxylate and backbone oxygens of Asp43 (one is hidden by the red arrow) and that is pointing its free electron pair in the direction of the **9** C_7 atom. The white dotted line indicates the proximity of Ser48 to the C_7 carbon of **9**. The drawing was made with PyMOL (http://pymol.sourceforge.net/).

simulations[16] using the minimized aldolase complexes as the starting point. Simulations sought to identify configurations of **9** in the active site that are consistent with incipient Schiff base formation, using a protocol previously described to analyze the reactivity of a **9** isomer, HNA-P, with rabbit muscle aldolase.[10] For all simulations, the reactive lysine residue was modeled in its nucleophilic form consistent with a pK_a of ~8 for Lys107 in the mammalian aldolase.[10] Energy minimizations yielded a stable Michaelis complex with **9**, free of close contacts, filling the entire active site cleft and necessitated the expulsion of only several water molecules in the crystal structure. Simulations of 5 ns duration for the parasite and mammalian aldolases showed the phosphate moiety to be persistently bound in its binding site, making identical electrostatic and hydrogen-bonding interaction with active site residues in both isozymes. We then analyzed the trajectories generated by the simulation for coordinate frames whose geometries are conducive for nucleophilic attack in *T. brucei* and rabbit muscle enzymes.[10] Only 3% of the frames analyzed displayed geometries consistent with nucleophilic attack by Lys116 in the *T. brucei* enzyme (Supporting Information). A representative frame is shown in Figure 4.

Notable is the reaction geometry in Figure 4 that places Lys116 nearly perpendicular to the aldehyde of **9** at a distance of 3.36 Å. This orientation is favorable for Schiff base formation in the first step of the inhibition mechanism. A similar percentage of frames (1.8%) suitable for nucleophilic attack by Lys107 was noted in the HNA-P Michaelis complex with mammalian aldolase.[10] Moreover, the intermolecular hydrogen bond between the hydroxyl and the aldehyde on the naphthalene skeleton of **9** (not shown in Figure 4) stabilizes the carbonyl group orientation for nucleophilic attack by Lys116. In model systems, the presence of a hydroxyl ortho to the aldehyde is

important for formation and Schiff base stabilization.[10] Surprisingly, no frame was found suitable for nucleophilic attack in the rabbit muscle aldolase simulation of the Michaelis complex with **9** and is consistent with poor reactivity by **9** in the mammalian isozyme. Although active sites differ in one residue (Gly302 in the mammalian enzyme being replaced by a bulkier Ala312 in *T. brucei* aldolase), analysis of dynamical trajectories did not reveal conformational differences in the positioning of **9** with respect to C_α atoms of these residues, suggesting that this amino acid change may not account for the observed reactivity differences. Reaction of **9** with the malarial aldolase whose active site composition is identical to that of mammalian aldolase would corroborate this conclusion.

The reactant configuration in Figure 4 places the γ-OH of Ser48 within van der Waals contact of the **9** carbonyl. Intriguingly, Ser48 oriented opposite and nearly perpendicular to the aldehyde would be well-positioned to interact with the nascent iminium ion and could be the residue that reacts with the Schiff base, leading to the final intermediate in the slow binding inhibition mechanism.

In conclusion, we have synthesized a selective time-dependent inhibitor of *T. brucei* aldolase that does not significantly inhibit mammalian aldolase activity. We identified Lys116 as being responsible for Schiff base formation. Molecular dynamics suggest that differences in stabilization of reaction geometries are responsible for the differential reactivity of **9** with *T. brucei* aldolase compared to rabbit muscle aldolase and that Ser48 is most likely the reactive residue in the second step of the inhibition mechanism. MS experiments performed on *L. mexicana* aldolase support these conclusions. Compound **9** and its "prodrug" analogues will be tested in in vitro cultures of *T. brucei* to determine if it causes growth retardation.

Acknowledgment. This work was funded by the European Commission, through its programs INCO-DC (Contract IC18-CT97-0220) and INCO-DEV (Contract ICA4-CT-2001-10075) to C.B. and P.A.M.M., and by a grant from the National Scientific Research and Engineering Council (NSERC) of Canada to J.S. We thank the Réseau Québécois de Calcul de Haute Performance (RQCHP) for computational resources for the molecular dynamical simulations. The authors are grateful to Professor J. Poupaert, Université Catholique de Louvain, Brussels, Belgium, for helpful discussions.

Supporting Information Available: Synthetic protocols, ^{1}H and ^{13}C NMR shifts, MS data and elemental analysis results of synthesized compounds, molecular biology and enzymology procedures, and molecular modeling. This material is available free of charge via the Internet at http://pubs.acs.org.

References

(1) World Health Organization report on Tropical Diseases Research (TDR) program (2002).
(2) (a) Howells, R. E. The modes of action of anti-protozoal drugs. *Parasitology* **1985**, *90*, 687−703. (b) Neujean, G. Chemotherapy and chemoprophylaxis of sleeping sickness caused by Trypanosoma gambiense. *Rev. Med. Liege* **1959**, *14*, 5−13.
(3) Milord, F.; Pepin, J.; Loko, L.; Ethier, L.; Mpia, B. Efficacy and toxicity of eflornithine for treatment of *Trypanosoma brucei* gambiense sleeping sickness. *Lancet* **1992**, *340*, 652−655.
(4) Sjoerdsma, A.; Schechter, P. J. Chemotherapeutic implication of polyamine biosynthesis inhibition. *Clin. Pharmacol. Ther*. **1984**, *35*, 287−300.
(5) Van Nieuwenhove, S. Clinical evaluation of eflornithine in Trypanosomiasis. *Trans. R. Soc. Trop. Med. Hyg*. **1985**, *79*, 692−696.
(6) (a) Visser, N.; Opperdoes, F. R. Glycolysis in *Trypanosoma brucei*. *Eur. J. Biochem*. **1980**, *103*, 623−632. (b) Verlinde, C. L.; Hannaert, V.; Blonski, C.; Willson, M.; Perie, J. J.; Fothergill-Gilmore, L. A.; Opperdoes, F. R.; Gelb, M. H.; Hol, W. G.; Michels, PAM. Glycolysis as a target for the design of new anti-trypanosome drugs. *Drug Resist. Updates* **2001**, *4*, 50−65.
(7) Opperdoes, F. R.; Baudhuin, P.; Coppens, J.; De Roe, C.; Edwards, S. W.; Weijers, P. J.; Misset, O. Purification, morphometric analysis and characterization of the glycosomes of the protozoan hemoflagallate *Trypanosoma brucei*. *J. Cell Biol.* **1984**, *98*, 1178−1184.
(8) Shu, B.; Barker, R. Fluorescence studies of the binding of alkyls and aryl phosphates to rat muscle aldolase. *J. Biol. Chem.* **1971**, *246*, 7041−7045.
(9) (a) Blonski, C.; Gefflaut, T.; Périé, J. Effects of chirality and substituents at carbon 3 in dihydroxyacetone-phosphate analogues on their binding to rabbit muscle aldolase. *Bioorg. Med. Chem*. **1995**, *3*, 1247−1253. (b) Gefflaut, T.; Blonski, C.; Perie, J. Slow reversible inhibitions of rabbit muscle aldolase with substrate analogues: synthesis, enzymatic kinetics and UV difference spectroscopy studies. *Bioorg. Med. Chem.* **1996**, *4*, 2043−2054. (c) Gefflaut, T.; Blonski, C.; Périé, J.; Willson, M. Class I aldolases: substrate specificity, mechanism, inhibitors and structural aspects. *Prog. Biophys. Mol. Biol*. **1995**, *63*, 301−340.
(10) (a) Blonski, C.; Moissac, D.; Perie, J.; Sygusch, J. Inhibition of rabbit muscle aldolase by phosphorylated aromatic compounds. *Biochem. J*. **1997**, *323*, 71−77. (b) Dax, C.; Coincon, M.; Sygusch, J.; Blonski, C. Hydroxynaphthaldehyde phosphate derivatives as potent covalent Schiff base inhibitors of fructose-1,6-bisphosphate aldolase. *Biochemistry* **2005**, *44*, 5430−5443.
(11) (a) Shoesmith, J. B.; Haldane, J. Condensation of diphenyl formamidine with phenol. Part I. A new synthesis of β-resorcy-aldehyde. *J. Chem. Soc*. **1923**, *123*, 2704−2707. (b) Shoesmith, J. B.; Aldane, J. Condensation of diphenyl formamidine with phenol. Part II. The general nature of the reaction. *J. Chem. Soc*. **1924**, *125*, 2405−2407.
(12) (a) Stowell, J. K.; Wildlanski, T. S. A new method for the phosphorylation of alcohols and phenols. *Tetrahedron Lett*. **1995**, *36*, 1825. (b) Ladame, S.; Claustre, S.; Willson, M. Selective phosphorylation on primary alcohols of unprotected polyols. *Phosphorus, Sulfur Silicon Relat. Elem.* **2001**, *174*, 37−47.
(13) Ginsburg, A.; Mehler, A. H. Specific anion binding to fructose bisphosphate aldolase from rabbit muscle. *Biochemistry* **1966**, *5*, 2623−2634.
(14) McCurdy, C. R.; Le Bourdonnec, B.; Metzger, T. G.; El Kouhen, R.; Zhang, Y.; Law, P. Y.; Portoghese, P. S. Naphthalene dicarboxaldehyde as an electrophilic fluorogenic moiety for affinity labelling: application to opioid receptor affinity labels with greatly improved fluorogenic properties. *J. Med. Chem*. **2002**, *45*, 2887−2890.
(15) (a) Tobias, P. S.; Kallen, R. G. Kinetics and equilibria of the reaction of pyridoxal 5′-phosphate with ethylenediamine to form Schiff bases and cyclic geminal diamines: evidence for kinetically competent geminal diamine intermediates in transimination sequences. *J. Am. Chem. Soc.* **1975**, *97*, 6530−6539. (b) McQuate, R. S.; Leussing, D. L. Kinetic and equilibrium studies on the formation of zinc(II) salicylaldehyde Schiff base derived from ethylenediamine and 1,3-diaminopropane. *J. Am. Chem. Soc*. **1975**, *97*, 5117−5125.
(16) (a) Weiner, S. J.; Kollman, P. A.; Case, D. A.; Singh, U. C.; Ghio, C.; Alagona, G.; Profeta, S. J.; Weiner, P. A. New force field for molecular mechanical simulation of nucleic acids and proteins. *J. Am. Chem. Soc*. **1984**, *106*, 765−784. (b) Weiner, S. J.; Kollman, P. A.; Nguyen, D. T.; Case, D. A. An all atom force field for simulation of proteins and nucleic acids. *J. Comput. Chem.* **1986**, *7*, 230−252.

JM050237B